Lin Li[1]
Centre for Ships and Ocean Structures (CeSOS),
Centre for Autonomous Marine Operations and Systems (AMOS),
Department of Marine Technology,
Norwegian University of Science and Technology (NTNU),
Trondheim NO-7491, Norway
e-mail: lin.li@ntnu.no

Wilson Guachamin Acero
Centre for Ships and Ocean Structures (CeSOS),
Centre for Autonomous Marine Operations and Systems (AMOS),
Department of Marine Technology,
Norwegian University of Science and Technology (NTNU),
Trondheim NO-7491, Norway

Zhen Gao
Centre for Ships and Ocean Structures (CeSOS),
Centre for Autonomous Marine Operations and Systems (AMOS),
Department of Marine Technology,
Norwegian University of Science and Technology (NTNU),
Trondheim NO-7491, Norway

Torgeir Moan
Centre for Ships and Ocean Structures (CeSOS),
Centre for Autonomous Marine Operations and Systems (AMOS),
Department of Marine Technology,
Norwegian University of Science and Technology (NTNU),
Trondheim NO-7491, Norway

Assessment of Allowable Sea States During Installation of Offshore Wind Turbine Monopiles With Shallow Penetration in the Seabed

Installation of offshore wind turbines (OWTs) requires careful planning to reduce costs and minimize associated risks. The purpose of this paper is to present a method for assessing the allowable sea states for the initial hammering process (shallow penetrations in the seabed) of a monopile (MP) using a heavy lift floating vessel (HLV) for use in the planning of the operation. This method combines the commonly used installation procedure and the time-domain simulations of the sequential installation activities. The purpose of the time-domain simulation is to quantitatively study the system dynamic responses to identify critical events that may jeopardize the installation and the corresponding limiting response parameters. Based on the allowable limits and the characteristic values of the limiting response parameters, a methodology to find the allowable sea states is proposed. Case studies are presented to show the application of the methodology. The numerical model of the dynamic HLV–MP system includes the coupling between HLV and MP via a gripper device, and soil–MP interaction at different MP penetration depths. It is found that the limiting parameters are the gripper force and the inclination of the MP. The systematic approach proposed herein is general and applies to other marine operations. [DOI: 10.1115/1.4033562]

Keywords: monopile installation, heavy lift vessel, initial hammering process, critical events, limiting parameters, allowable sea states

1 Introduction

The installation of OWTs is costly due to the challenging environmental conditions and a large number of wind turbine units need to be installed. To better prepare the operations and increase the weather windows during the planning phase, systematic and practical methodologies for assessing this kind of operations are needed.

MP are the most commonly used foundations in water depths up to 40 m. It was reported that by the end of 2013 more than 75% of all installations are supported on MPs [1]. The installation of a MP wind turbine includes the erection of the MP, transition piece, tower sections, and rotor and nacelle assembly. This study focuses on the installation of the MP which in general includes the following steps: upending and lowering, and driving/drilling operations. After arrival on site, the MP is upended from a transportation barge or the crane vessel and lowered through water so that it is standing vertically on the seabed. A hydraulic hammer is placed on top of the pile and used to drive it into the seabed to a predetermined depth. In case a rocky subsurface prevents driving operations, a drilling bit is inserted into the pile to drill through the substrate [2]. The installation can be carried out using jack-ups which provide stable working platforms for the installation, but their application is limited to a maximum water depth around 45 m [3] and the lowering of the jack-up legs is time-consuming and requires low-sea states. Floating vessels, on the other hand, have more flexibility for offshore operations and are effective in mass installations of a wind farm due to fast transit between foundations. However, the motion of floating vessels affects the responses of the installation system and brings more challenges for load transfer operations.

There are very few publications dealing with the MP installation. Previous studies have been focused on proposing new installation methods and developing more accurate numerical methods to increase the installation weather window. Sarkar and Gudmestad suggested a method to install MP by isolating the installation operations from the motion of the floating vessel using a preinstalled submerged support structure [4]. They showed that the overturning moment on the structure during MP hammering was the limiting parameter for MP installation. The dynamic responses of a coupled HLV–MP system during the lowering process of the MP were studied in Ref. [5]. The performance using both a floating vessel and a jack-up was also compared in their study. Furthermore, Li et al. introduced a method to account for the shielding effects (crane vessel shelters the MP from the wave action) during the entire lowering operation of the MP [6]. The vessel reduces the wave kinematics at its leeward side and thus the wave forces on the MP. It was concluded that when accounting for the shielding effects, the responses obtained from the numerical analysis can be greatly reduced in short waves by selecting a proper heading of the vessel. The approach was further

[1]Corresponding author.

Contributed by the Ocean, Offshore, and Arctic Engineering Division of ASME for publication in the JOURNAL OF OFFSHORE MECHANICS AND ARCTIC ENGINEERING. Manuscript received December 21, 2015; final manuscript received April 20, 2016; published online June 1, 2016. Assoc. Editor: Yi-Hsiang Yu.

studied and extended to compare the performance during lifting of a MP and a jacket OWT foundation, respectively [7]. Recommendations regarding the heading angles of the vessel during the lifting operations of the two OWT substructures were given. In addition, the importance of radiation damping of the MP during the nonstationary lowering operation was examined in Ref. [8]. A new approach was proposed to account for radiation damping in the time-domain numerical simulation of the nonstationary lowering process. This study showed that accounting for the radiation damping on the large diameter MPs can reduce the responses of the lifting system and may increase the allowable sea states especially for short wave conditions.

As it is shown above, most of the previous research on the MP installation primarily focused on the numerical modeling of different installation activities and calculation of dynamic responses. However, for offshore installations, it is of great importance to establish the operational limits in a pragmatic way based on installation procedures and proper identification of critical and restricting events. The procedure for the MP installation is well known by offshore installation contractors. To identify the critical events for the whole installation, numerical analysis are required to study the dynamic responses of each sequential installation activity. Each critical event has a limiting parameter and corresponding allowable limit, e.g., structural failure of hydraulic cylinders due to extreme contact forces which are limited by the allowable working loads. However, the severity of these critical events can be reduced by mitigation actions by modifying the operational procedure and by upgrading the equipments to increase the allowable limits. Thus, a systematic identification of the critical events and the corresponding parameters to describe these events (limiting parameters) is necessary to plan the operation, i.e., establish operational limits for installation, propose contingency actions, and select the equipment in a cost-effective manner. Moreover, it is useful to have the operational limits in terms of environmental conditions (sea states, wind, and current), and this is the main purpose of this study.

This study proposes a systematic approach for predicting allowable sea states based on installation procedures and coupled HLV–MP dynamic responses during MP installation at shallow seabed penetrations (in this paper also known as initial MP hammering process), which is a critical phase for MP installation. First, a general description of the MP's hammering procedure is given. Second, coupled HLV–MP dynamic model is established and used in steady-state time-domain simulations for incremental seabed penetration depths. Based on the numerical results, the critical events and corresponding limiting parameters are identified. Then, a systematic procedure to obtain the allowable sea states for such operations is proposed. To demonstrate the method, case studies are conducted. Finally, conclusions are made and possible future work is presented.

2 MP Hammering Procedure and Critical Events

The system components and general MP hammering procedure are given in this section. Then, based on this procedure, a preliminary assessment of the critical events and their limiting parameters is given.

2.1 System Components. The system setup for the MP hammering process is illustrated in Fig. 1. The system is composed of HLV, MP foundation, hammer, and gripper device. The common design of the gripper device includes several hydraulic cylinders. By varying the stroke length of the cylinders, the gripper is able to correct the mean inclination of the MP during the initial hammering process. The numerical modeling of the coupled system is discussed in detail in Sec. 4. The main particulars of the system components are shown in Table 1.

2.2 General MP Hammering Procedure. After an initial self-penetration into the seabed, the MP is supported vertically by the soil and laterally by the gripper device. Then, the main lift wire is released. The commonly applied hammering procedure is described in the following steps.

(1) *Place the hammer onto the MP's top*: The hydraulic lines are connected to the hammer, which is then lifted from the HLVs deck and placed onto the MP. The weight of the hammer increases the MP's self-penetration depth and moment of inertia and modifies the dynamic properties of the system.
(2) *Measure and correct the mean inclination of the MP*: Current and wave forces normally cause an initial mean inclination of the MP which could be increased further at deeper penetrations if the hammering process starts without any correction. The conventional way to measure the

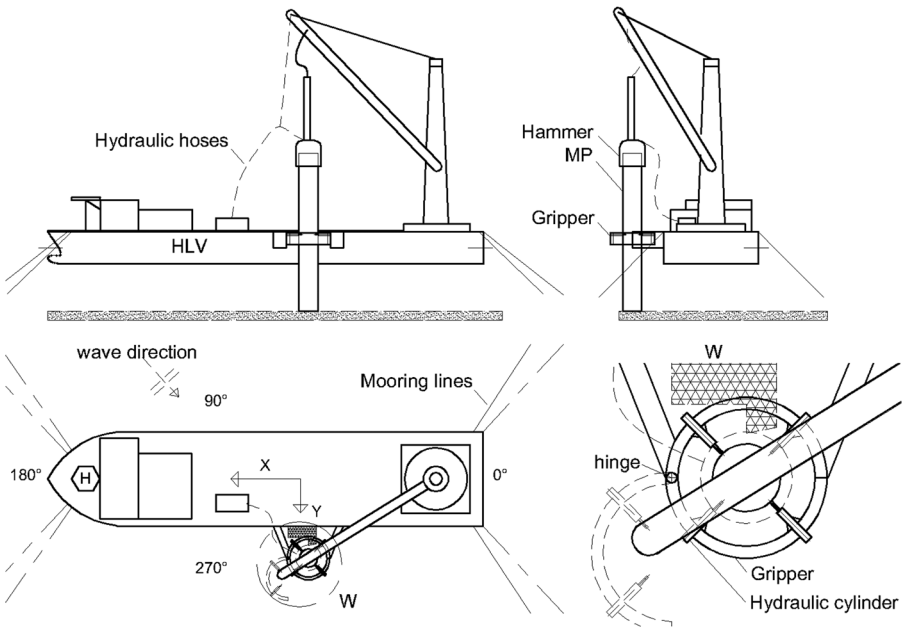

Fig. 1 System setup for the MP hammering process

Table 1 Structures' main particulars

Parameter	Notation	Value	Units
–HLV			
Displacement	∇	5.12×10^4	Ton
Length	L	183	m
Breadth	B	47	m
Draught	T	10.2	m
Metacentric height	GM	5.24	m
Vertical position of COG above keel	VCG	17.45	m
–MP			
Mass	M_{MP}	500	Ton
Diameter	D_{MP}	5.7	m
Length	L_{MP}	60	m
–Hammer			
Mass	M_{Hammer}	300	Ton

verticality of the MP is using a handhold inclinometer on the outer surface of the pile. Due to the first- and second-order vessel-induced motions and the irregularity of the pile surface, multiple measurements are required to ensure the accuracy. Despite this fact, the uncertainties of the measurements are relatively large. A new measurement method based on the visual object recognition combined with vessel motion compensation is expected to increase the accuracy of vertical measurement and also the efficiency of the operation [9]. The corrections of MP inclination can be done using hydraulic cylinders on the gripper by varying the pressure in the cylinders to change the stroke length, see Fig. 1.

(3) *Precompress the hydraulic cylinders and hammer a few number of blows*: Once the mean inclination is corrected, the hydraulic fluid supply valves are closed to keep the internal pressure, and a precompression force is applied to allow the cylinder rods to be in contact with the MP at all times to avoid gaps and subsequent impact loads. Corrective control of MP inclination is possible if the contact forces are not beyond the capacity of the hydraulic cylinders and the mean inclination is small. Therefore, during the initial hammering process, only a few (around three) blows are given. The penetration rate of the MP depends on the soil conditions, and decreases with increasing depth. After each inclination correction, the hammer does not start immediately. There is a time interval between each correction and hammering activities, e.g., the time spent on preparation for hammering and waiting time between each blow. During this time interval, the HLV–MP system moves continuously in waves. Thus, the following hammer blows create a new MP inclination which depends on the motions of the system and the length of the time interval after the correction. This step lasts around 10 min.

(4) *Measure MP's inclination and correct it using hydraulic cylinders:* After each hammering operation, correction of the mean MP inclination is required to avoid cumulative inclination angles prior to the next hammering. The hydraulic cylinders are only able to provide force to correct the inclination before the soil resistance becomes too large. An average time using inclinometers to measure the inclination will be less than 10 min.

(5) *Repeat step 3 and 4 until the hydraulic cylinders are not able to correct the MP's inclination*: The previous two steps are repeated until the MP penetrates a few meters into the soil. At a certain stage, it is not possible to correct the MP's inclination by only using hydraulic cylinders.

(6) *Correct the inclination using thrusters and varying mooring line tension*: Due to the high resistance from the soil, the hydraulic cylinders cannot correct the mean inclination of the MP. Therefore, it is necessary to apply the available thruster forces and change the mooring line length. These external forces will change the mean position of the vessel and they are transferred to the hydraulic cylinders which correct the mean inclination of the MP. A typical maximum combined thruster and mooring external force is around 400 kN for a HLV with characteristics used in this study.

(7) *Retract the hydraulic rods and drive MP to the final penetration*: When the MP is stabbed deep enough into the soil, its inclination cannot be corrected due to soil resistance. The hydraulic rods are retracted. The MP is then driven to its final penetration. The inclination of the MP before retracting the rods determines the final inclination of MP since no corrections can be applied afterward. This final piling could last less than 30 min depending on the soil properties. Note that a successful operation will require the system to be intact and the inclination to be acceptable before this activity.

The flowchart of the MP hammering procedure is shown in Fig. 2. The initial hammering process is defined in the flowchart which includes the hammering–measuring–correcting activities before retracting the rods of the hydraulic cylinders. The focus of this paper is on the initial hammering process.

2.3 Critical Events and Limiting Parameters. The possible critical events and limiting parameters from the initial hammering process (see Fig. 2) that may lead to an unsuccessful operation are summarized as follows.

- *Failure of the hydraulic system*. The extreme force on the hydraulic system may exceed the allowable values. These forces include the dynamic component due to HLV–MP dynamic motions and the static component which is required for the correction of the mean inclination of the MP. The exceedance of the allowable forces on the system will result in a hydraulic system failure and it is a critical event because it will not only stop the operation but also may pollute the environment if leakage of the hydraulic fluid occurs. The corresponding limiting parameter is the total force on individual hydraulic cylinder including the dynamic contact force and

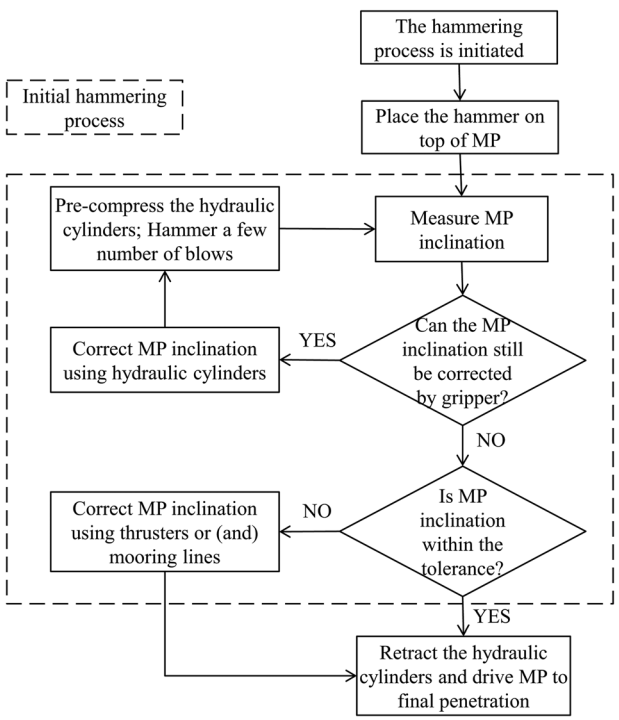

Fig. 2 Flowchart of the MP hammering procedure

correction force. The probability of exceeding the allowable working forces should be kept small enough to ensure a sufficient safety margin.

- *Insufficient thruster and mooring line forces available*. The thruster and mooring lines may provide insufficient forces during the final correction of the MP's mean inclination. If the HLV is a dynamic positioning (DP) vessel, the thrusters are used to compensate the environmental forces and also to provide force to correct the mean inclination of the MP. When the penetration depth and the MP mean inclination are large, the extra static force required to correct the inclination can make the total forces exceed the thrusters' capacity. On the other hand, if only mooring lines are used to correct the MP inclination, the required tensions may not be applied. The limiting parameters for this event are the available thruster force and mooring line tension.
- *Unacceptable MP inclination*. MP inclination may exceed the allowable limit and result in an unsuccessful installation, and the typical limit is below 1 deg [10]. Because the hydraulic system and the thrusters are not able to correct the inclination of the MP after a certain penetration, the maximum inclination of the MP before retracting the hydraulic cylinders determines the final inclination of the MP. This event is not critical but restrictive for the installation requirement and its limiting parameter is the MP inclination due to the coupled HLV–MP motions.

The critical events and limiting response parameters differ if new procedures or equipment are employed. In this study, the thruster and mooring line capacity are assumed to be sufficient during the hammering phase and are not considered as limiting parameters in the numerical analysis. No structural damage on the MP due to gripper contact forces is assumed. In addition, the failure of the hydraulic system is driven by the extreme axial force exceeding the allowable design value, and the lateral loads are assumed secondary. A summary of the hammering process activities, critical events, limiting parameters, and allowable limits are listed in Table 2. For each activity, a preliminary estimation of the operational duration is given as reference for weather window analysis.

3 Methodology to Establish the Allowable Sea States

According to DNV-GL recommendations [11], the design and planning phases of marine operations shall evaluate allowable environmental conditions when the operations can be carried out and provide weather criteria for starting and interrupting the operations. In order to do this, the installation procedure and numerical models are used to identify potential restricting and critical events of the various sequentially defined installation activities. For these events, the corresponding limiting parameters are then identified. Next, characteristic responses need to be calculated from frequency- and/or time-domain analyses. By comparing the characteristic values of the limiting parameters at different environmental conditions with the allowable values, the allowable sea states can be found.

As discussed earlier, the initial hammering process finishes when the thrusters and the hydraulic cylinders cannot correct the inclination of the MP. The allowable sea states must ensure that the hydraulic system is intact and MP inclination is acceptable at this installation stage. The methodology proposed here requires the introduction of new parameters. Here let us define two "critical penetration depths":

- d_{c1}: the penetration depth at which the MP can stand alone in the soil without any support from the vessel.
- d_{c2}: the penetration depth at which the hydraulic cylinders and thrusters are not able to correct the MP inclination;

To ensure a safe hammering operation, it is necessary to satisfy:

$$d_{c2} \geq d_{c1} \tag{1}$$

which requires the hydraulic cylinders to be able to support the MP until it can stand alone in the soil. Therefore, it is necessary to identify d_{c1} during the planning phase, and to calculate the extreme forces on the hydraulic cylinders when the penetration depth is less than d_{c1}. It will be shown later in the paper that the forces on the hydraulic cylinders increase significantly with increasing penetration depths, so it is beneficial to retract the cylinder rods upon reaching d_{c1}. In this paper, the completion of the initial hammering process is achieved when the MP's penetration depth reaches d_{c1}. d_{c1} is calculated by evaluating the responses of the MP in relevant sea states supported only by soil at various penetration depths (MP–soil interaction model refers to Sec. 4.1.3). In practice, safety factors should be included to ensure that the MP can stand alone in waves at this penetration depth.

The following procedure is then proposed to find the allowable sea states (see Fig. 3).

- For a given sea state, the first step is to calculate the "critical penetration depth" d_{c1} for which the MP (and the hammer on top) can stand in the soil for this sea states without any external supports from the HLV.
- Then, the force on the individual hydraulic cylinders which is the limiting criterion in the first several hammering actions is calculated. The extreme force should include both the dynamic force due to HLV–MP relative motions and the one required to correct the MP from a certain inclination to zero mean value. The limiting force criterion should be checked for each penetration depth less than d_{c1} to make sure the operation is acceptable for the subsequent activities. If the requirement fails at any penetration, the input sea state is

Table 2 Screening of MP sequential hammering activities, critical events, and corresponding parameters to describe the events (limiting parameters)

No.	Activity	Duration [min]	Critical event	Limiting parameter
1	Place the hammer onto MPs top	45	/	
2	Measure and correct the inclination of the MP	20	/	
3	Precompress the hydraulic cylinders and hammer a few number of blows	10	/	
4	Measure MP inclination and correct it using hydraulic cylinders	10	failure of hydraulic system	individual hydraulic cylinder force
5	Repeat step 3 and 4 N times while it is possible to correct the MPs inclination	20*N	failure of hydraulic system	individual hydraulic cylinder force
6	Correct the inclination using thrusters and varying mooring line tensions	10	failure of hydraulic system, insufficient thruster capacity, mooring line failure, MP inclination not acceptable	individual hydraulic cylinder force, thruster force, mooring line tension, MP inclination
7	Retract the hydraulic rods and drive to final penetration	30	/	

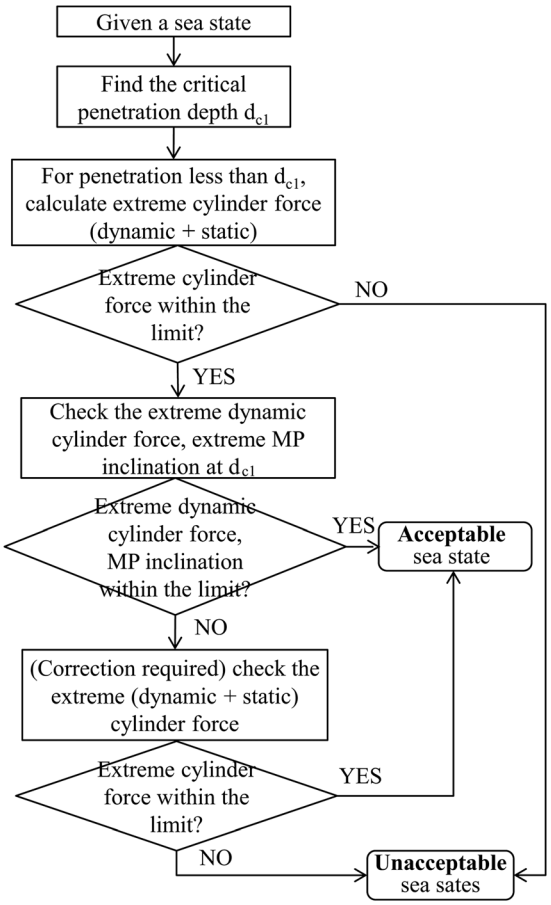

Fig. 3 Methodology to find the allowable sea states for the initial hammering process

considered "unacceptable," and a lower sea state should be selected and evaluated.

- When reaching d_{c1}, the hydraulic cylinder rods are about to be retracted. If both the dynamic cylinder forces and MP's inclination at d_{c1} are within the limits, the given sea state is acceptable without any further correction of the MP inclination. On the other hand, if the MP inclination exceeds the allowable value, further correction is required. Thus, the total correction and dynamic force on the hydraulic rods are calculated and it is acceptable if the total force is below the allowable values.

When assessing the operational limits, a probabilistic approach should be applied to take into account the uncertainties in measurements of the MP inclination, the extreme value estimates of the contact forces, soil parameters of the offshore site, numerical models, and human errors. However, this study was simplified and these uncertainties were not considered. Based on the proposed procedure, the allowable sea states for a given installation site can be derived in the planning phase. In order to evaluate the responses of the system, a reliable numerical model for the hammering process is required. In addition, proper allowable values for different limiting parameters must be established. Before giving examples to find the allowable sea states, the numerical modeling of the dynamic system as well as its characteristic responses are studied in Sec. 4.

4 Modeling and Analysis of Global Dynamic Responses of the Coupled HLV–MP System

In this section, the numerical models used to investigate the responses of the coupled HLV–MP system at various seabed penetration depths are given to properly identify critical events and develop the methodology that was proposed in the Sec. 3 (see Fig. 3).

The time-domain simulations provide the dynamic global responses of the HLV–MP system in the steady-state condition at different penetration depths. Here, the steady-state condition means that for each time-domain simulation, the mean draft of the vessel and the mean penetration depth of the MP do not change with time, and the wave realization follow a stationary distribution. The hammering operation itself (involving impact forces from the hammer blows) is not modeled. The hammering operation could happen at any time instance during the dynamic process when the MP moves horizontally at the gripper connection level. As a result, a new mean inclination angle of the MP is created. It is assumed that the soil force acts through the MP center. The hammer impact does then not affect this mean inclination because the impact and the MP are perfectly aligned. The hydraulic cylinders are then used to correct the mean inclination before the next hammering operation. The correction phase is the most critical one because the forces on the hydraulic cylinders include both the dynamic component from the coupled HLV–MP motions and the actual correction force. Thus, the total contact force during the correction phase can be decomposed as the correction force from quasi-static analysis (see Sec. 5.2) and the dynamic force from the steady-state time-domain simulations in this section.

Furthermore, a sensitivity study on the effect of soil properties on the dynamic responses of the system with different soil properties is carried out in Sec. 4.3.

4.1 Theory and Methodology for Numerical Modeling and Analysis. The numerical model for this study was built using the MARINTEK SIMO program [12]. The model includes the coupled two-body HLV–MP system with mooring line positioning system on the HLV and soil interaction forces on the MP at different penetration depths. The methodology for the modeling and the time-domain simulation are explained in detail in Secs. 4.1.1 to 4.1.3.

4.1.1 Equations of Motion for Coupled Dynamic Analysis. The HLV–MP-coupled dynamic system has 12 degrees-of-freedom (DOFs), and for each body, the following six equations of motion are solved in the time-domain.

$$(\mathbf{M}+\mathbf{A}(\infty))\ddot{\mathbf{x}}+\mathbf{D}_1\dot{\mathbf{x}}+\mathbf{D}_2 f(\dot{\mathbf{x}})+\mathbf{K}\mathbf{x}+\int_0^t \mathbf{h}(t-\tau)\dot{\mathbf{x}}(\tau)d\tau = \mathbf{F}_{\text{ext}}(t)=\mathbf{q}^{(1)}{}_{\text{WA}}+\mathbf{q}^{(2)}{}_{\text{WA}}+\mathbf{F}_{\text{moor}}+\mathbf{F}_{\text{cpl}}+\mathbf{F}_{\text{soil}} \quad (2)$$

where, $\mathbf{M}$ is the mass matrix, $\mathbf{x}$ is the rigid-body motion vector of the body with 6DOFs, $\mathbf{A}$ is the frequency-dependent added mass matrix, and $\mathbf{D}_1$ and $\mathbf{D}_2$ are the linear and quadratic damping matrices. The viscous effects from the vessel hull and the mooring system were simplified into linear damping terms in surge, sway, and yaw. The roll damping of the vessel as well as the quadratic damping on the MP was also included. Additionally, $\mathbf{K}$ is the hydrostatic restoring matrix from the HLV and the MP; $\mathbf{h}$ is the retardation function calculated from the frequency-dependent added mass or potential damping coefficients and $\mathbf{F}_{\text{ext}}$ is the external force vector, including the first-order wave excitation forces, $\mathbf{q}^{(1)}{}_{\text{WA}}$, the second-order wave excitation forces, $\mathbf{q}^{(2)}{}_{\text{WA}}$, the mooring line forces on the HLV, $\mathbf{F}_{\text{moor}}$, the coupling forces between the HLV and MP, $\mathbf{F}_{\text{cpl}}$, and the soil reaction forces on the MP, $\mathbf{F}_{\text{soil}}$. The second-order wave excitation forces were obtained based on the Newman's approximation and include only the difference-frequency slowly varying forces [13]. The eight catenary mooring lines for the HLV were also modeled, and both a quasi-static analysis and a simplified dynamic analysis accounting for the effect of drag loading on the lines were applied.

It should be noted that this numerical model only accounts for wave loads on the HLV and MP. The mean wind and current speed will only create mean displacement, but the turbulence in

wind may also provide dynamic loads. For this specific system with floating vessel and MP, the dynamic responses are governed by wave loads. Therefore, the effects from both wind and current are not considered.

The hydrodynamic interaction between the HLV and MP affect the wave excitation forces, the added mass, and damping coefficients. In the current model, the hydrodynamic interactions mainly affect the forces on the MP due to the vessel presence, which is considered as "shielding effects" since the MP is a small structure compared with the HLV. The shielding effects from the vessel on the MP were studied during the nonstationary lowering operation when installing the MP in Ref. [6] by using interpolation of wave kinematics to calculate the wave forces on the MP. However, in the current numerical case the mean wet surface of the MP did not change during the simulation, and two panel models were built and the hydrodynamic interaction problems were solved using the panel method program WAMIT [14] in the frequency domain. In the time-domain simulations, the effects on the wave excitation forces are included in the external forces on the right hand side of Eq. (2) by applying force transfer functions from WAMIT, while effects on frequency dependent added mass and damping forces are included in the coupled retardation functions.

Step-by-step integration methods are applied to calculate the responses of the coupled HLV–MP system using an iterative routine. The equations of motion are solved using Newmark-beta numerical integration ($\beta = 0.1667, \alpha = 0.50$) with a time step of 0.01 s. The first-order and second-order wave forces are pregenerated using the fast Fourier transformation at the mean position of the HLV and the MP. The gripper coupling, mooring, as well as the soil–MP interaction forces are calculated in the time-domain. Short-crested waves with index $n = 3$ for the spreading function $\cos^n$ is applied for all sea states [15].

4.1.2 Modeling of the Gripper Device. The gripper device is normally a ring-shaped structure with several hydraulic cylinders in a radial array which provide pressure and thus compression forces on the MP during the initial hammering process. In the numerical model, the gripper device was simplified by four fender components with chosen stiffness and damping coefficients. When the MP tends to move away from the gripper, the fenders provide compression forces and limit its horizontal motions. Figure 1 shows the gripper model and the elastic model for the gripper contact elements are illustrated in Fig. 4. Sensitivity studies to quantify the effects of the gripper stiffness on the responses during the lowering of a MP were performed in Ref. [5]. The study showed that the contact force and the relative motion between the MP and the gripper device were very sensitive to the gripper stiffness.

In this study, the parameters for the gripper are chosen based on specifications of typical hydraulic cylinders which are applied in practice for MP installation. During the hammering process, the valves of the hydraulic cylinders are normally closed. Because of the elasticity of the fluid oil, the hydraulic cylinder behaves like a mechanical spring. The stiffness of the spring was calculated according to Ref. [16] and depends on the fluid elasticity, the area of the piston and the total compression volume for the fluid. Damping is caused by friction in the actuator and the pipe system. By using technical data of hydraulic cylinders, the stiffness of the cylinder with closed valves was found to be about 10^7–10^8 N/m, and was chosen to be 3×10^7 N/m in the current model. The damping in the numerical model is taken to be 20% of critical damping which is a reasonable value for hydraulic cylinders [16].

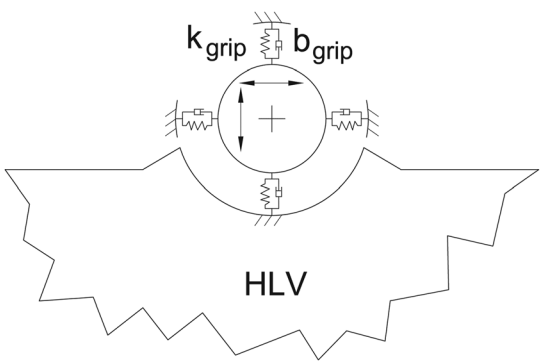

Fig. 4 Elastic model of the gripper contact elements

It was also found from the numerical simulations that if an initial gap between the gripper and the MP is applied, huge impact forces will occur as compared to the case with a zero initial gap [6]. Because of the large inertia of the MP, initial gaps allow the MP to accelerate and the velocities at contact with the gripper increases. A good strategy is to provide zero gap with proper precompression forces to avoid gaps and consequently huge impact forces. In the current model, a precompression force of 150 kN for each hydraulic cylinder is applied.

4.1.3 Soil–MP Interaction. The soil–structure interaction model is important for the global dynamic analysis of structures embedded in soil. Most of the relevant studies of the soil–MP interaction focus on installed piles, and not during the installation phase. For offshore structures, the foundation piles are normally subjected to axial, lateral, and overturning loads. The method normally used to model the soil–pile interaction under these loads is based on the Winkler modeling approach with combination of *p–y* curves, see e.g., Refs. [17–21]. This method assumes that the pile acts as a beam supported by a series of uncoupled springs, each of which represents the local soil reaction forces. These springs are described by nonlinear functions (*p–y* curves) to define the soil reaction force, *p*, at a given depth, as a function of the lateral displacement, *y* [22,23]. The *p–y* curves for offshore structures are based on the results of field tests on long slender piles, with diameters around 610 mm and a large length to diameter ratio of 34 [24].

The conventional *p–y* method was extended for large diameter MPs by including additional soil reaction terms [24,25]. Four separate components of soil reaction were included in the proposed design model: the traditional distributed *p–y* curve, the distributed moment curve due to the vertical shear (skin friction) around the pile, the base shear curve, and the base moment curve [24]. Results from 3D finite-element parametric studies on large piles with diameters from 5 m to 10 m indicated that *p–y* curve features were dominant for the long piles (length to diameter ratio is 6) while the other three factors were negligible. However, for short piles (length to diameter ratio is 2), these additional terms became more significant, especially the distributed moment due to the friction between the soil and the pile [24]. For the initial hammering process with soil–MP model at shallow penetrations, the length to diameter ratio is less than 2. Therefore, both the *p–y* curve and the distributed moment should be accounted for.

Besides the stiffness modeled by nonlinear springs, the soil damping needs to be considered to study the dynamic behavior of the system. Soil damping comes in two main sources: radiation damping and hysteretic material damping. Radiation damping is negligible for frequencies less than 1 Hz [17]. Therefore, the main contribution for the current model is from the hysteretic material damping. The material damping can be estimated from a hysteresis loop created by loading and unloading *p–y* curves [26].

In this study, the soil–MP interaction is modeled using the extensively applied Winkler model by means of distributed springs and the hysteresis material damping. The penetration of the MP during the initial hammering process ranges from around 2 m (self-penetration) to around 6–8 m (depending on soil properties) after which the gripper can not correct the MP inclination. The soil–MP interaction forces in the shallow penetration phases are three-dimensional; therefore, the 2D Winkler model is extended to 3D by using nonlinear springs distributed in both axial and circumferential directions along the MP. The distributed

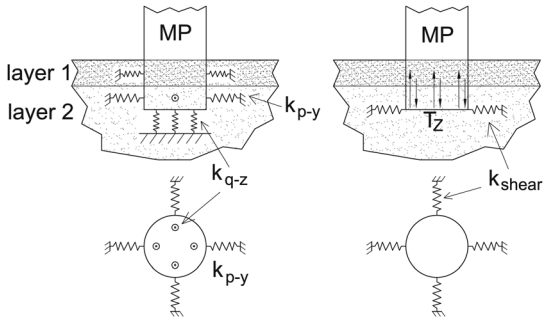

Fig. 5 Numerical models for the soil–MP interactions

springs include the traditional lateral load-deflection p–y curve, the friction T–z curve which was found to be significant for large diameter piles with shallow penetrations [24], the base shear curve, and the tip load–displacement Q–z curve.

The configuration of the springs as shown in Fig. 5 is summarized as follows: four vertical springs K_{q-z} to model Q–z curves at the bottom of the MP; four springs T_z on the side of the MP to model the T–z curve for the friction force from both inside and outside wall of the MP, and the vertical position of the T_z springs are calculated by considering the distribution of the friction along the whole MP penetration length. For p–y curves, the whole penetration is divided into several 2 m-layers, and four circumferential springs K_{p-y} are applied for each layer. On the bottom of the MP, four springs K_{shear} are used to model the shear resistance force. The number of the distributed spring is considered to be sufficient since the MP bottom tip will experience small displacement (less than 10 cm for typical sea states).

An estimate of the stiffness for all the nonlinear distributed springs shown in Fig. 5 is taken from the API guideline [23]. The API approach is pertinent to the small diameter flexible piles and it underestimates the soil reaction at the top of large diameter MPs [18,27,28]. From Ref. [24], it was found that API and FEM methods result in different load–displacement curves. The differences are, however, important for site specific soil types and vary even in the same field. In this paper, the methodology is general and intended to cover typical soil parameters ranging from soft to hard soil, so that it would be applicable to any soil whose properties fall within the ranges considered here. Furthermore, from the sensitivity study on the soil properties in this paper in Sec. 4.3, it is concluded that the dynamic system behavior during the operation does not change with the soil properties. Therefore, representative values for the nonlinear springs for the soil–MP interactions are considered to be sufficient for this study. In addition, the cyclic loading effects, such as accumulation of deformation and degradation, are not considered. The soil properties used to calculate the spring stiffness are shown in Table. 3. As mentioned earlier, the soil damping is included in this model in terms of dynamic friction force. A typical soil reaction moment and MP inclination curve under cyclic loads in the current MP–soil interaction model are shown in Fig. 6.

4.2 Dynamic Response of the HLV–MP System at Different Penetration Depths. The purpose of the time-domain simulations is to identify the limiting parameters and critical events. The numerical model was established using MARINTEK SIMO program [12] and was verified with the one built in ANSYS AQWA [30] from where consistent results were obtained. To compare the responses of the MP in different installation stages, five penetration depths of the MP were considered, i.e., 2 m, 4 m, 6 m, 8 m, and 10 m. The condition with HLV free floating is also included for comparison against the coupled HLV–MP dynamic responses at various loading conditions. The dynamic responses from the time-domain simulations include the motions of the HLV–MP system, and forces from the coupling in the gripper, the mooring lines of the HLV as well as the soil–MP interaction. The results presented in this section allow better understanding of the dynamic system behavior toward identifying the limiting parameters. The characteristic values of the limiting parameters to determine the allowable sea states are evaluated later in Sec. 5.

Figure 7 compares the responses of the HLV in free floating (HLV-only) and the HLV coupled with the MP at different penetration depths. This figure displays the standard deviations (STD) of the HLV motions in 6DOFs with respect to its COG. The responses at different wave peak periods show different trends when the penetration of the MP changes. In general, the motions of the HLV in the vertical plane (heave, roll, and pitch) change little at different penetration depths. The roll motion decreases slightly with increasing MP penetrations because of the stiffness and damping contributed from the soil–MP interaction. When the wave peak period increases, the motions in the vertical plane increase due to increasing first-order resonant motions of the HLV in long waves.

On the other hand, the motions in the horizontal plane (surge, sway, and yaw) show large variations for different loading conditions. In short waves, the surge and sway motions decrease rapidly with increasing penetrations. However, in long waves the motions first decrease and then increase for larger depths (8 m and 10 m). The yaw motion of the vessel increases rapidly with the wave period.

Similarly, the responses of the MP inclination vary greatly with the MP penetration as observed in Fig. 8. The first row in Fig. 8 shows the *STD* of the MP inclination and the second row shows the *STD* of the individual hydraulic cylinder contact force. The reason why the horizontal motions of the HLV–MP system show different characteristics in short and long waves is the change of the natural modes periods of the system with the coupling between HLV and MP at different penetration depths. This can be seen from the response spectra at different conditions.

Figures 9–11 show the response spectra of the surge and sway motion of the gripper, the yaw motion of HLV at two wave peak period conditions. The gripper motions were calculated based on the HLV motions according to the following equation:

$$\mathbf{s} = (\eta_1 + z\eta_5 - y\eta_6)\hat{i} + (\eta_2 - z\eta_4 + x\eta_6)\hat{j} + (\eta_3 + y\eta_4 - x\eta_5)\hat{k} \tag{3}$$

where η_1 to η_6 are the 6DOF rigid body motions of the HLV and (x, y, z) is the position of the gripper in the HLV body-fixed coordinates, which is $(x = -10\,\text{m}, y = 30.0\,\text{m}, \text{and}\, z = 10.0\,\text{m})$. Since the x and z positions of the gripper are close to the HLV COG while it is 30 m away from the HLV in y coordinate, the yaw motion of the HLV greatly affects the surge motion of the gripper.

Table 3 Soil properties applied in the numerical model (refer to Ref. [29])

layer	Type	Submerged unit weight (kN/m^3)	Internal friction angle (deg)	Unit skin friction (kPa)	Unit tip resistance (kPa)
0—2 m	sand	10	36	20	1900
2—4 m	sand	10	36	24.8	2300
4—6 m	sand	10	37	39.1	3400
6—8 m	sand	10	35	51.4	3700
8—10 m	sand	10	35	51.4	3700

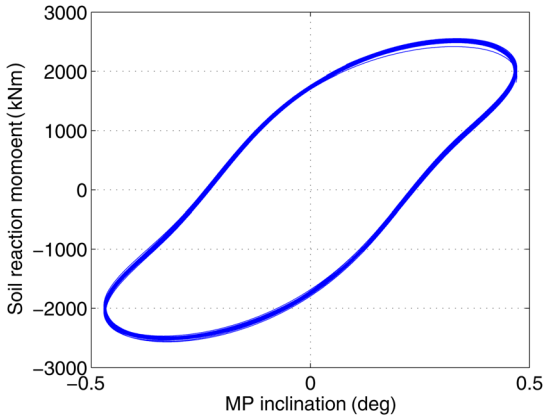

Fig. 6 Typical soil reaction moment versus MP inclination due to cyclic loading with period of 6 s

The natural frequencies of the moored HLV alone are around 0.1 rad/s for surge and sway and around 0.2 rad/s for yaw. In contrast, for the coupled HLV–MP system, different modes are identified. The system properties change with MP penetration depth, and the dynamic responses vary with wave conditions.

In short waves with $T_p = 5\,s$, the surge, sway, and yaw motions for different MP penetrations are dominated by the second-order motions of the vessel. For sway, the peak frequencies shift to the higher values and the amplitudes decreases with increasing penetrations (see Fig. 10(*a*)). This is because of the increase on the contribution from the soil–MP interactions. For surge and yaw motions, the response modes are more complicated. The original modes for yaw and surge of the HLV change when the HLV is coupled with MP (see Fig. 9(*a*), both surge and yaw contributes to the gripper surge motion), and the yaw rotation center is shifted from the COG of the HLV toward the MP due to large gripper and soil stiffness. As a result, the surge and yaw motions of the HLV have large coupling and two modes are observed: one mode with surge and yaw in phase and the other mode with surge and yaw

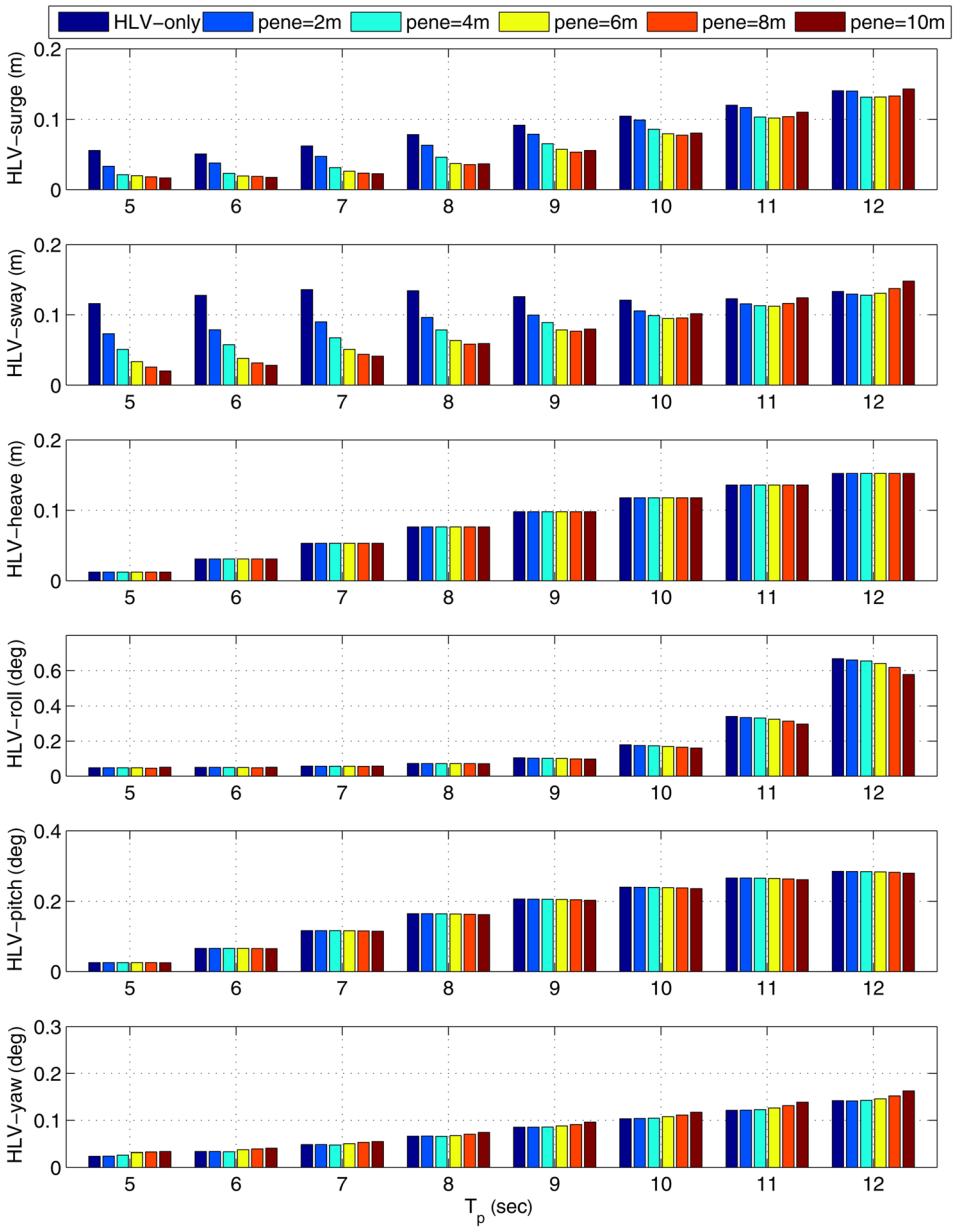

Fig. 7 Standard deviations of HLV motions at different MP penetration depths (*pene*) and wave conditions from 3-hr time-domain simulations ($H_s = 1.5$ m, $Dir = 150$ deg)

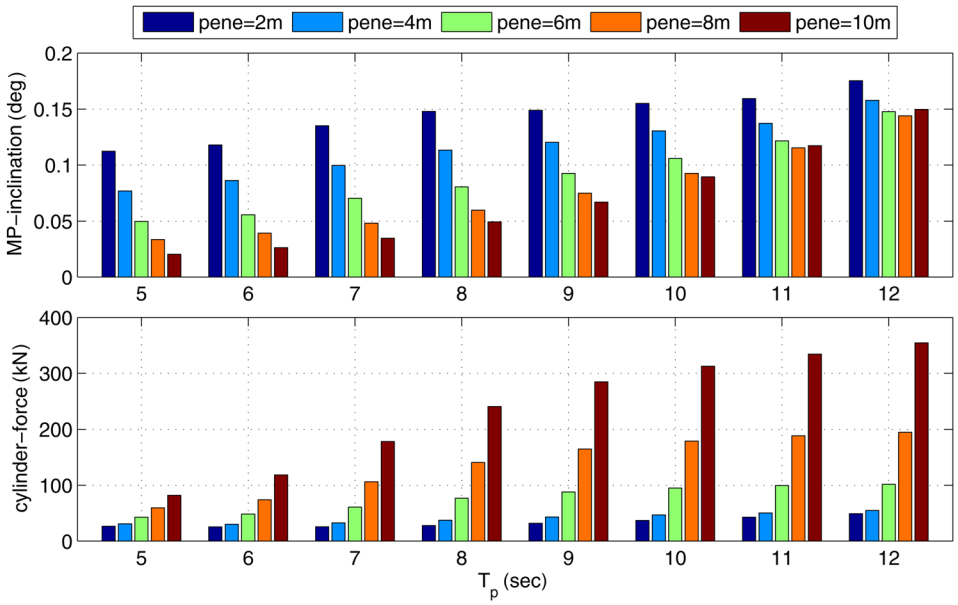

Fig. 8 Standard deviations of MP inclinations and contact forces on one hydraulic cylinder at different MP penetration depths (*pene*) and wave conditions from 3-hr time-domain simulations ($H_s = 1.5$ m, $Dir = 150$ deg)

out of phase. The natural frequency of the second mode increases rapidly with MP penetration and become close to the peak frequencies of long waves (see Fig. 11(*b*)).

With the increase of the wave peak period, the first-order motions of the vessel increase. For shallow penetrations, the second-order motions are still dominating, while for deeper penetrations the first-order motions dominate the total responses (see Fig. 9(*b*)). Since the natural period of the motions in deeper penetrations are closer to the wave peak periods compared to those in the shallow penetration cases, the first-order motions increase with the penetration (see Fig. 9(*b*) bottom). Therefore, the total motions begin to increase in long waves when the first-order motions dominate (e.g., Fig. 7 top). The increase of gripper surge motions are the most significant because of the contributions from both surge and yaw motions of the HLV. The cylinder contact forces keep increasing with the penetration and wave period as shown in Fig. 8. The spectra of the force on one hydraulic cylinder are shown in Fig. 12. For both short and long waves, the first-order responses dominate for penetrations larger than 4 m. The second-order components contribute in short wave conditions, especially when the MP penetration is small. Due to the significant increase of the soil stiffness with penetration depth, the gripper force in general follows the same trend for different wave conditions. The cylinder contact force may exceed the design forces when the MP is deep in the soil and the wave period is large, and it is beneficial to retract the cylinder rods to avoid huge cylinder forces at larger soil penetration depths.

From the dynamic responses above, it is clear that the MP can reach unacceptable inclination angles during normal operational conditions, and the cylinder contact forces may exceed the

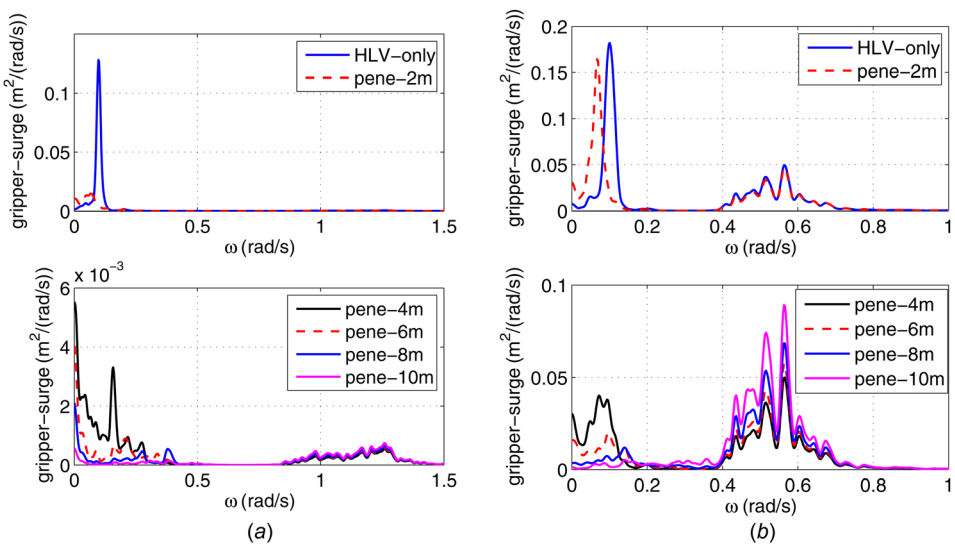

Fig. 9 Response spectra of the gripper surge motion for two different wave peak periods at different MP penetration depths (*pene*): (*a*) $H_s = 1.5$ m, $T_p = 5$ s, $Dir = 150$ deg and (*b*) $H_s = 1.5$ m, $T_p = 10$ s, $Dir = 150$ deg

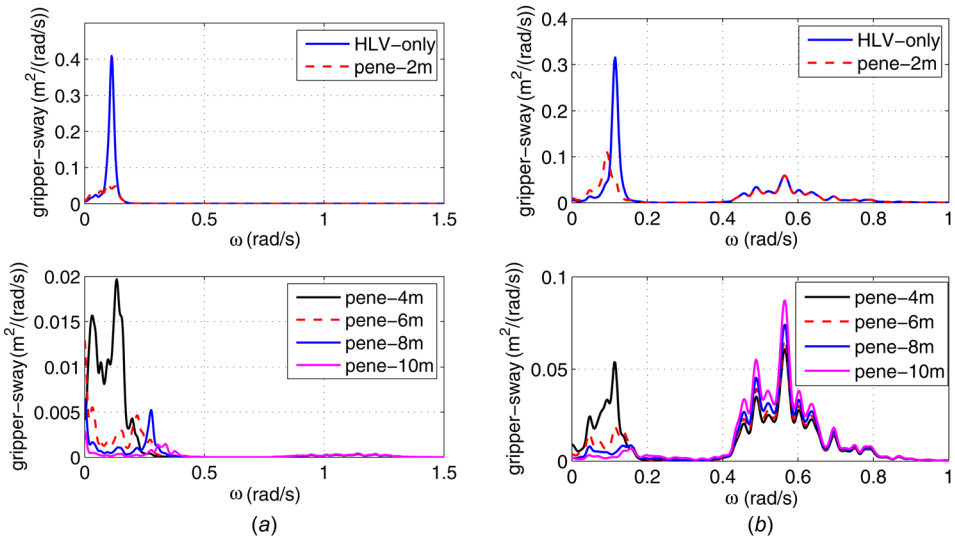

Fig. 10 Response spectra of the gripper sway motion for two different wave peak periods at different MP penetration depths (*pene*): (*a*) $H_s = 1.5$ m, $T_p = 5$ s, *Dir* = 150 deg and (*b*) $H_s = 1.5$ m, $T_p = 10$ s, *Dir* = 150 deg

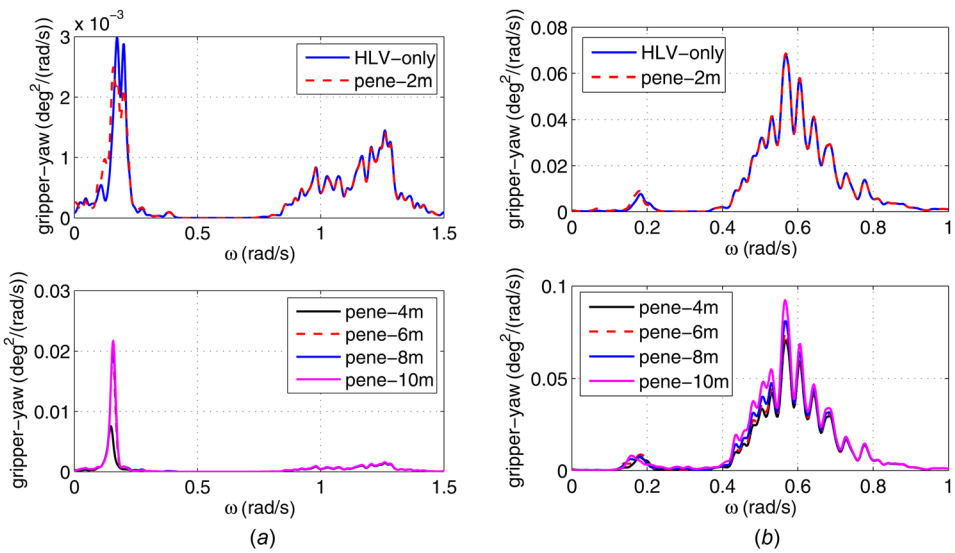

Fig. 11 Response spectra of the HLV yaw motion for two different wave peak periods at different MP penetration depths (*pene*): (*a*) $H_s = 1.5$ m, $T_p = 5$ s, *Dir* = 150 deg and (*b*) $H_s = 1.5$ m, $T_p = 10$ s, *Dir* = 150 deg

allowable working limits. Thus, both MP inclination and cylinder contact force are considered to be "limiting parameters" of the initial hammering process.

For comparison, the hydraulic cylinder forces when using a jack-up are shown in Fig. 13. Because little motion of the jack-up in waves and high stiffness of the gripper device, the inclination of the MP is negligible in all conditions, and the cylinder contact forces are in general smaller compared with using the floating vessel. The cylinder force decreases with wave periods and change little with the MP penetration depth. Since the jack-up is a fixed platform, the gripper and the soil are only required to counteract the wave excitation forces on the MP which decreases with wave periods. The increase of the penetration depth only changes the boundary condition of the MP and does not affect the wave excitation force. The cylinder contact force in short waves are observed larger when using a jack-up than using the floating vessel at shallow MP penetration. This is because the shielding effect reduces the MP excitation force when employing the floating vessel, while no shielding effect exists from the jack-up vessel [6]. The comparison shows that the limiting parameters for floating vessel installation activities are not considered critical when using a jack-up vessel. The critical activity for a jack-up is during the installation and retrieval phases, i.e., the phases when the legs are being set down onto and lifted up from the seabed. The critical event due to the impacts from vessel motions in waves and "punch through" the soil is the consequent failure of the structural components, see e.g., Refs. [3,31].

4.3 Sensitivity Study on the Soil Properties and Effects on the Dynamic System Behavior. To generalize the methodology to different site conditions, sensitivity studies are performed using three soil properties. The chosen soil properties cover most of the sandy soils for shallow penetrations. The stiffness of the

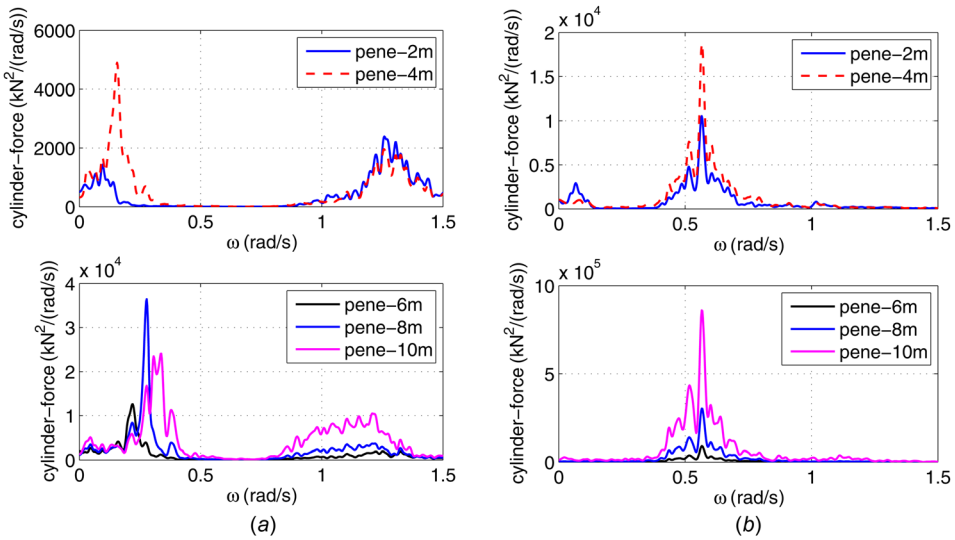

Fig. 12 Response spectra of the hydraulic cylinder force for two different wave peak period conditions at different MP penetration depths (*pene*): (*a*) $H_s = 1.5$ m, $T_p = 5$ s, *Dir* = 150 deg and (*b*) $H_s = 1.5$ m, $T_p = 10$ s, *Dir* = 150 deg

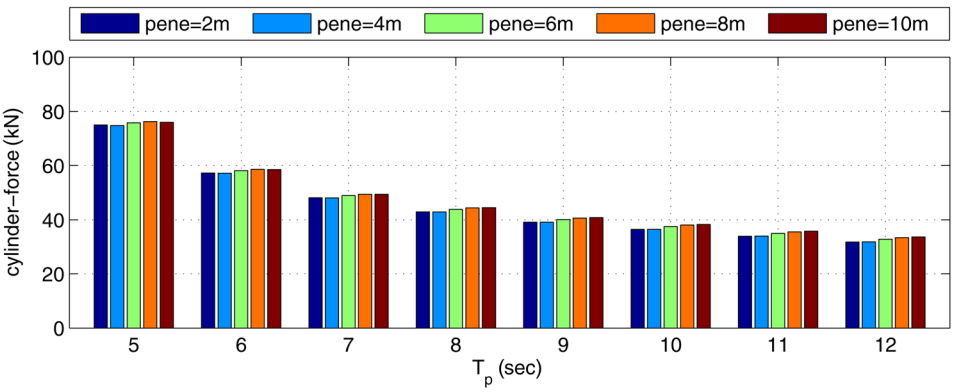

Fig. 13 *STD* of hydraulic cylinder contact forces at different MP penetration depths (*pene*) when using a jack-up vessel ($H_s = 1.5$ m, *Dir* = 150 deg)

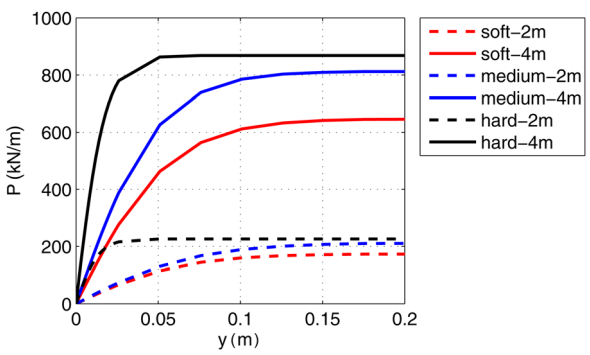

Fig. 14 *p–y* curves for different soil types

distributed springs K_{p-y}, T_z, K_{q-z}, and K_{shear} as shown in Fig. 5 increases from soft soil to hard soil, and here only the representative *p–y* curves for three soil properties at two penetrations are shown in Fig. 14. Dynamic analysis of the HLV–MP–soil system is performed in different sea states with MP at various penetrations, and the modeling parameters for the sensitivity study are shown in Table 4.

Figure 15 displays the relation between the individual cylinder contact force versus the MP inclination, which was found to be the limiting parameter for this operation. The results using different soil properties with MP at various penetrations are included in the same figure. The axes are the maximum inclination and maximum contact forces which are used to evaluate the allowable sea states. The procedure followed for calculation of the maximum values is explained in Sec. 5.

Table 4 Parameters for sensitivity study on the soil properties

	Soil identity	Type	MP penetration	Sea states
1	Soft soil	sand	2 m, 4 m, 6 m, 8 m	$H_s = 2$ m, $T_p = 6$ s; $H_s = 1.6$ m, $T_p = 8$ s
2	Medium soil[a]	sand	2 m, 4 m, 6 m, 8 m	$H_s = 2$ m, $T_p = 6$ s; $H_s = 1.6$ m, $T_p = 8$ s
3	Hard soil	sand	2 m, 4 m, 6 m	$H_s = 2$ m, $T_p = 6$ s; $H_s = 1.6$ m, $T_s = 8$ s

[a]The properties for medium soil refer to Table 3.

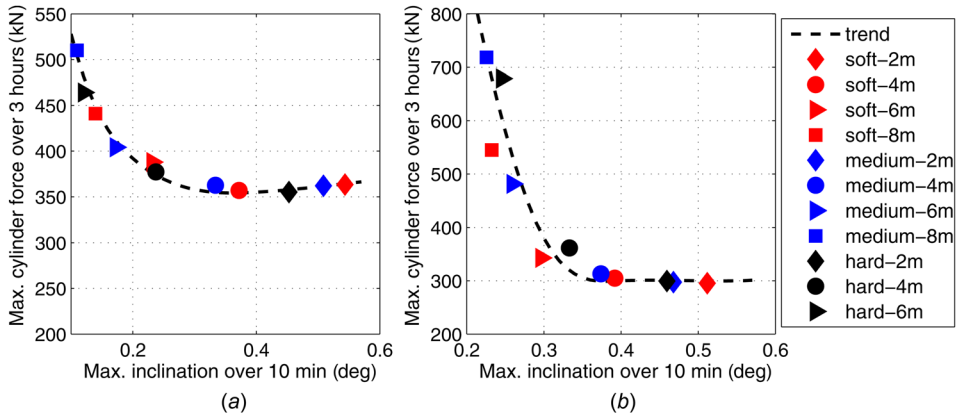

Fig. 15 Extreme cylinder force in 3 hrs versus MP maximum inclination in 10 min for different sea states and soil properties at different penetrations: (*a*) $H_s = 2$ m, $T_p = 6$ s and (*b*) $H_s = 1.6$ m, $T_p = 8$ s

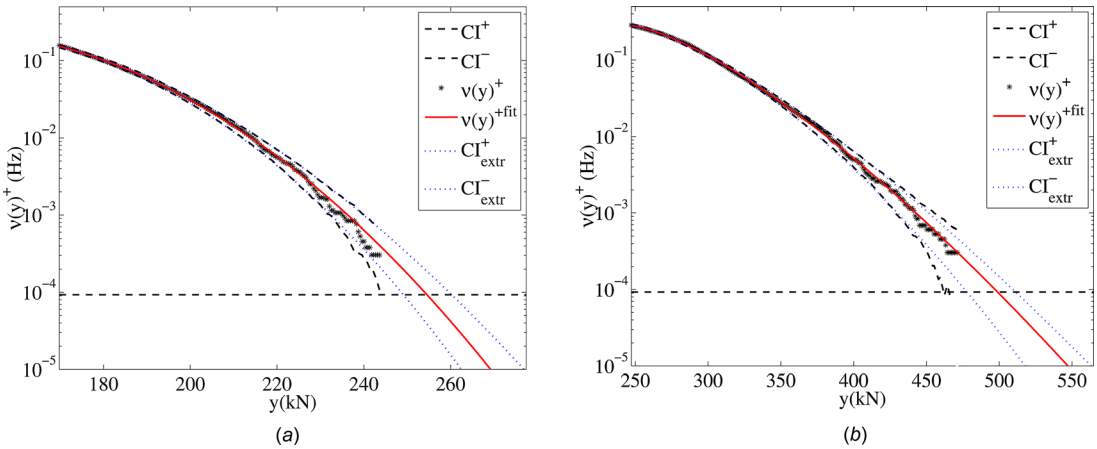

Fig. 16 Mean upcrossing rate of the hydraulic cylinder force using 20 samples. Legends: time-domain simulation (·), curve fitting (–), empirical 95% confidence band (CI – – –), smooth confidence band ($\mathrm{CI_{extr}}$ · · ·): (*a*) $H_s = 1.5$ m, $T_p = 6$ s, *pene* = 4 m and (*b*) $H_s = 1.5$ m, $T_p = 10$ s, *pene* = 6 m

For a given soil property, Fig. 15 shows that the contact force and the MP inclination at different MP penetrations follow a trend. It can be observed from the figure that for both sea states, the contact force increases while the MP inclination decreases in deeper seabed penetrations. For different soil types, the force–inclination relation follows the same trend as shown in Fig. 15. Although, the maximum forces for $H_s = 1.6\,m$, $T_p = 8\,s$ scatter more at higher penetrations, the results show good consistency in the force–inclination trend and therefore in the dynamic system behavior. Thus, it is evident that the force–inclination relation is not sensitive to the soil properties. For a given allowable limit of the contact force, the MP inclination for different soils is the same, but the critical penetrations corresponding to the limiting force are different—it is deeper in soft soil than in hard soil. In other words, the allowable sea states do not depend on the soil types, but the critical penetration depth to retract the hydraulic cylinders d_{c1} (see Fig. 2) varies with soil properties.

Thus, the methodology proposed to assess the operational limits for this operation can be generalized for different soil conditions. In addition, this sensitivity study also proves that the soil weakening effects due to cyclic loads may change the critical penetration depth, but the maximum contact force and corresponding MP inclination are not influenced. Therefore, to identify the limiting parameters and develop methodology to establish the allowable sea states for the MP initial hammering operation, it is sufficient to use representative soil properties. In the following case studies, the "medium soil" (see Table 4) is applied for all sea states.

5 Case Study on Allowable Sea States

The purpose of this section is to apply the proposed systematic methodology for preliminary assessment of the allowable sea states via numerical examples. The characteristic values of the limiting parameters, i.e., the cylinder contact force and the MP inclination are first obtained based on numerical simulations. The corresponding allowable limits are also presented and followed by typical case studies on allowable sea states.

5.1 Extreme Dynamic Forces on Hydraulic Cylinders. The extreme total force on the hydraulic cylinder includes the dynamic force from the steady-state conditions which is presented in this subsection and the correction force during the correcting phase which is discussed in Sec. 5.2.

In this study, the extreme dynamic forces are calculated as the maximum value in 3 hrs, corresponding to a probability of exceedance of around 10^{-4}. This value is chosen to ensure structural integrity and is commonly used for marine operation activities [11]. In practice, the equipment should be sized based on the required number of installations, and the extreme forces used for selecting the equipment should be consistent with its service life. Besides,

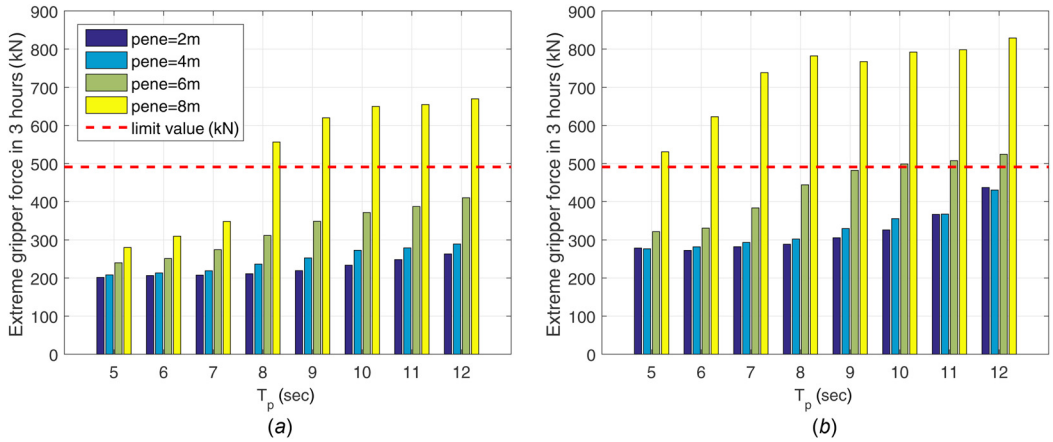

Fig. 17 Extreme cylinder forces in 3 hrs at different penetration depths (*pene*): (*a*) $H_s = 0.8$ m, Dir = 150 deg and (*b*) $H_s = 1.5$ m, *Dir* = 150 deg

possible sources of uncertainties (e.g., the environmental conditions) need to be included in terms of safety factors. However, it is out of the scope of this study.

The extreme dynamic force on the gripper is estimated from the steady-state time domain simulations using the empirical mean upcrossing rates. The upcrossings of high threshold limits are statistically independent events, and thus a Poisson probability distribution is assumed adequate for the extreme values [32]. The cumulative distribution function of the extreme value $M(T)$ of the response process during the time T is then given by [33]

$$P(M(T) \le y) = \exp\left(-\int_0^T \nu_y^+(t)dt\right) \tag{4}$$

where ν_y^+ denotes the positive mean upcrossing rate of the level y, which is defined as the frequency of passing the level y. ν_y^+ is found from time-domain simulations, and extrapolation is required for low upcrossing rates values. The extrapolation strategy proposed in Ref. [34] is applied.

Figure 16 shows two examples of the fitting and extrapolation of the cylinder forces with low and high extreme values, respectively. One clearly sees that the present upcrossing method follows the empirical points appropriately. The confidence interval of 95% is also shown to estimate the deviation of the results. The 3-hr extreme values for different sea states are obtained using this method and presented in Fig. 17. The extreme values in this figure are obtained using ten samples of 40-min simulations. As shown, the extreme dynamic forces increase significantly and nonlinearly with both penetration depth and wave height.

5.2 MP Inclinations and Correction Forces. As mentioned, after every hammering operation before reaching the critical depth d_{c1} at which the MP can stand alone in waves, the mean inclination of the MP should be corrected using hydraulic cylinders. This mean MP inclination is created by the hammer blows when the HLV–MP system experiences wave-induced motions. During the correction phase, the total force on the hydraulic cylinder includes the dynamic forces induced by the waves and a correction force when changing the cylinder's rod length and mooring line tensions for correction of the MP inclination. As mentioned, in the numerical model the total correction force, F_c, is decomposed as a dynamic and a correction component. The dynamic force in waves during the correction is consistent with the one at steady-state condition with zero mean inclination and the extreme dynamic value is obtained from Fig. 17. The correction force is then calculated here by excluding the waves.

Figure 18 illustrates the phase between each hammering activity. After each correction, the mean MP inclination is zero (Fig. 18(*a*)). Due to the dynamic motions of the HLV–MP system, after the hammer blows the MP has a mean inclination angle Ω_1, and the penetration depth increases from d_1 to d_2 (Fig. 18(*b*)). The hammer blows do not influence this mean inclination because it is perfectly aligned with the MP. The soil is assumed to be in intact condition after each hammering activity for MP mean inclination

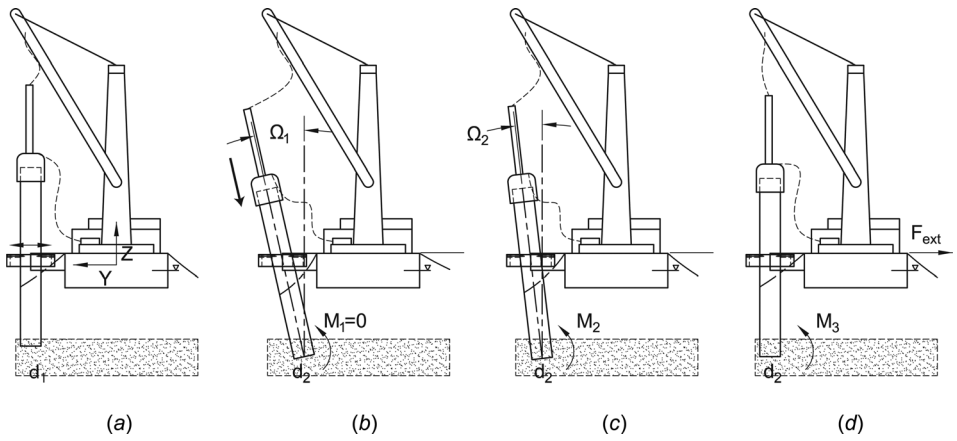

Fig. 18 Illustration of the phases between hammering activities: (*a*) system mean position before hammering, (*b*) system position after hammering, (*c*) system equilibrium mean position after hammering, and (*d*) system mean position after correction

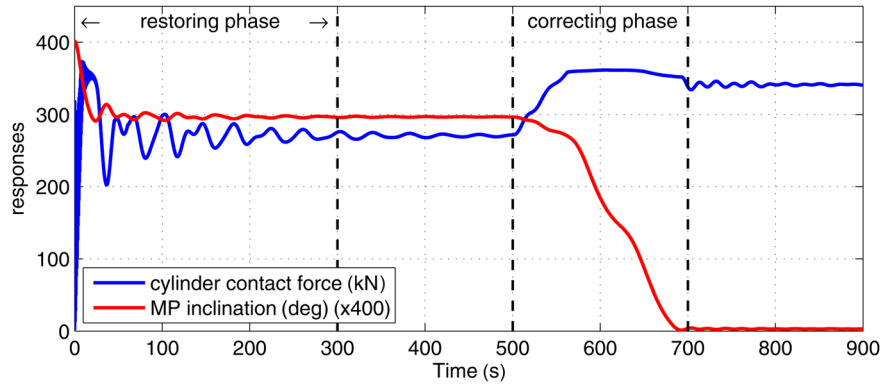

Fig. 19 Responses of the HLV–MP coupled system after hammering and during the correction phase (corresponds to Figs. 18(*b*) to 18(*d*))

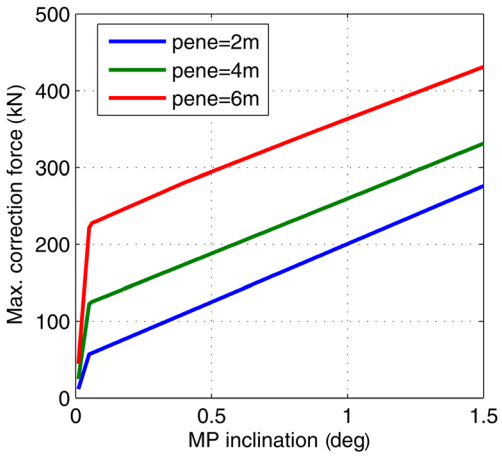

Fig. 20 Correction forces at different penetration depths (*pene*) and initial mean inclinations

Ω_1, so the soil reaction moment is $M_1 = 0$. Meanwhile, the HLV has an offset from its mean position, and its mooring lines tend to restore the vessel toward its mean position and the MP inclination is reduced. The soil reaction force and the mooring line tension reach equilibrium at the MP mean inclination angle Ω_2 with soil reaction moment M_2 (Fig. 18(*c*)). The phase from inclination angle Ω_1 to Ω_2 is considered to be mooring line "restoring phase." Then, by applying external forces on the system F_{ext}, the mean inclination angle Ω_2 is corrected to a zero mean value (Fig. 18(*d*)).

During the correction phase with MP mean inclination from Ω_1 to Ω_2 and further to 0, the maximum correction forces on the hydraulic cylinders are used together with the extreme dynamic forces in waves to calculate the total extreme forces on the hydraulic cylinders. The cylinder contact force at any inclination angle Ω_i between Ω_1 and 0 deg needs to overcome the soil reaction forces and the inertial moment at Ω_i. The soil reaction force is calculated using the model shown in Fig. 5, with initial intact condition at MP inclination Ω_1. Then, the approach to estimate the correction forces here is conservative.

Figure 19 shows an example on the responses of the coupled HLV–MP system during the restoring and correction phases (corresponds to Figs. 18(*b*)–18(*d*)) at MP penetration depth of 6 m and an initial mean inclination angle from hammering $\Omega_1 = 1$ deg. The results in Fig. 19 are for heading sea condition (while Fig. 18 illustrates the case for beam seas). During the "restoring phase," the MP mean inclination decreases from 1 deg to around 0.75 deg and the cylinder force also decreases due to decreasing friction force from the soil. Next, by applying external forces at time instant 500 s, the cylinder contact force begins to increase to overcome the soil reaction force and the MP inclination decreases to zero. The maximum force from this process is taken as the correction force, and Fig. 20 presents the correction force for different penetration depths and initial mean inclination Ω_1.

As shown, the correction force increases significantly with the initial inclination angle Ω_1 from the hammer blows. As discussed earlier, Ω_1 depends on the coupled HLV–MP motion as well as the time interval between the end of the previous correction and the end of each hammering activity. This time interval is considered to be less

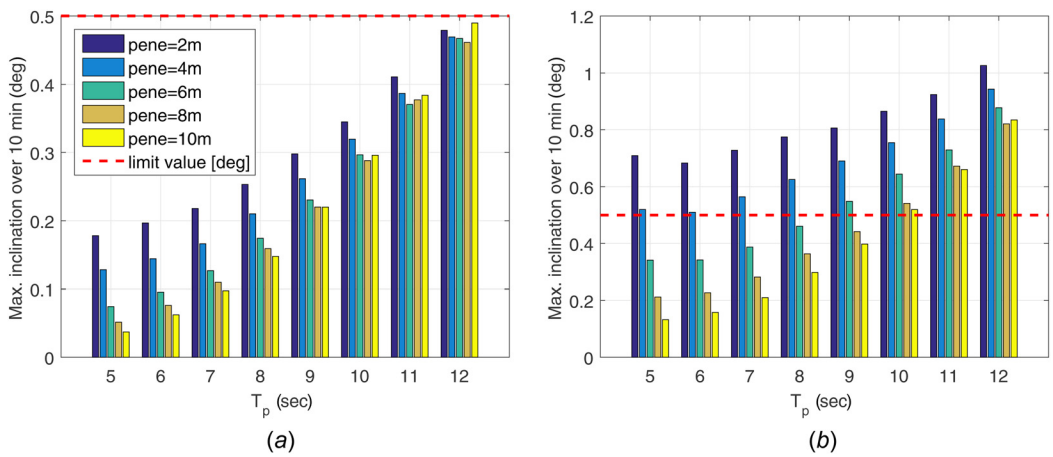

Fig. 21 Maximum MP inclination over 10 min at different penetration depths (*pene*): (*a*) $H_s = 0.8$ m, Dir = 150 deg and (*b*) $H_s = 1.5$ m, *Dir* = 150 deg

than 10 min (refer to Table 2). Therefore, the maximum inclination over 10 min is applied as the characteristic value for Ω_1 to obtain the correction force using Fig. 20, while the probability of exceedance of 10^{-4} (used for the characteristic cylinder forces) is not applicable because the inclination will not lead to structural failure. Similarly, the final inclination of the MP in the initial hammering process is also chosen as the maximum value over 10 min after the last correction. Figure 21 shows the 10-min maximum inclinations in different conditions. The inclination increases significantly with both T_p and H_s. In lower sea states with $H_s = 0.8\,m$, the inclination is below the limit value, but corrections are still required for a penetration less than the critical penetration depth to avoid cumulative inclinations.

5.3 Case Studies. In this study, the mechanical components of the gripper and their configuration were selected based on the most common designs used in the industry. Assuming the rod diameter of the hydraulic cylinder is around 140 mm, according to the technical data for 100 bar cylinders, the limiting force is around 491 kN [35].

Piling tolerances are set by combining a number of aspects. The governing factor is the tolerance on the lower flange of the turbine tower. In most cases, this is 0.1 deg. Counting back from this, combining it with the maximum correction that can be made with a transition piece or shims, the tolerance for the inclination of the piles is set. The values are normally between 0.5 deg and 1 deg for MPs [10]. In the case study, 0.5 deg is applied as the allowable limit for MP inclinations.

Figure 22 demonstrates four typical cases when determining the limiting sea states based on the proposed methodology. These cases include three unacceptable sea states and one acceptable case. The reasons for the different cases to occur in terms of the coupled HLV–MP motions are explained as follows.

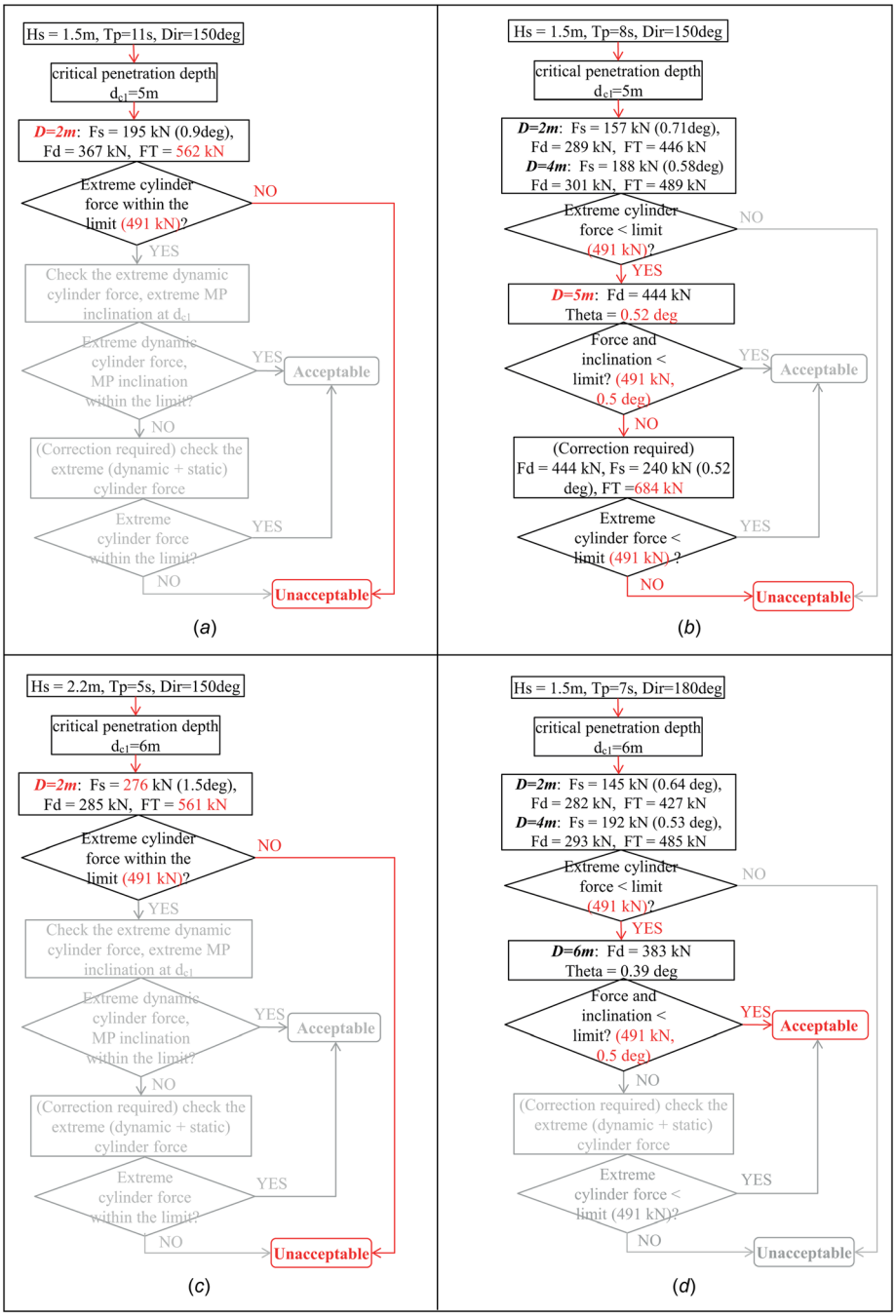

Fig. 22 Case studies: (*a*) case 1, (b) case 2, (c) case 3, and (d) case 4

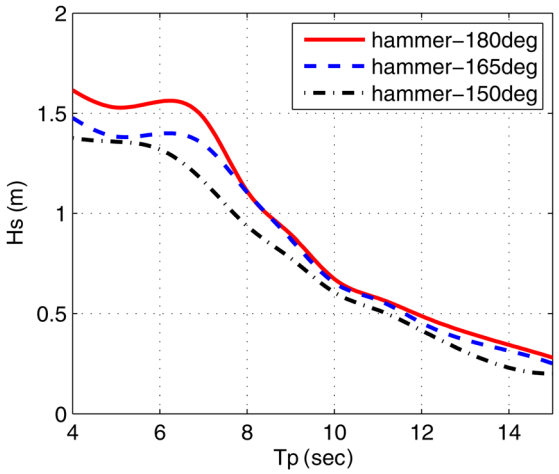

Fig. 23 Allowable sea states for MP initial hammering operation for typical HLV headings

- *Case 1*: The given sea state does not satisfy the criterion at the beginning of the hammering process ($pene = 2$ m) because of large cylinder forces. Both dynamic and static correction forces are significant due to the first-order resonant motions of the HLV–MP system in long waves. The motions of the HLV in vertical plane increase in long waves as the wave peak frequencies move close to its natural frequencies.
- *Case 2*: The wave period in this case is shorter than in Case 1 and the motions are also smaller. So the operation is acceptable before reaching the critical penetration depth d_{c1}. However, the MP inclination at d_{c1} exceeds the allowable limits, and the last correction using thrusters (or mooring lines) are required. Because of large soil resistance, the total force on the gripper exceeds the limits when applying the correction at d_{c1} which makes the given sea state unacceptable.
- *Case 3*: As indicated in Sec. 4.2, in short wave conditions, the motions of the vessel are mainly due to the second-order slow-varying motions in the horizontal plane. These motions may result in large correction forces for the MP in shallow penetrations, e.g., at 2 m. Compared to the previous cases with long wave periods, Case 3 occurs at relatively higher H_s since inclinations due to the second-order motions in short waves are less significant compared to inclinations due to first-order resonant motions in long waves with the same significant wave height as shown in Fig. 21.
- *Case 4*: With wave periods shorter than Cases 1 and 2, and lower significant wave heights than Case 3, both first and second-order motions of the coupled system are in reasonable range, so the cylinder forces and the inclination lie within the limits and thus the input sea state is acceptable.

Therefore, the different reasons for the unacceptable sea states can be identified from the case studies, and different strategies could be proposed to reduce the responses or mitigate critical events accordingly. By assessing different wave conditions, the allowable sea states can be obtained. Figure 23 shows the results corresponding to three typical installation heading angles of the HLV based on the numerical models presented in this paper. As shown here, the allowable sea states for MP hammering operation can be predicted by applying a systematic methodology to all possible environmental conditions during the planning phase. The allowable sea states can be used to support the on board decision-making together with the weather forecast, e.g., to make decisions on whether to initiate the hammering operation as shown in Fig. 2.

6 Conclusions and Recommendations

The current work deals with the vessel–MP coupled system during the initial hammering process. Because offshore installations require proper planning and execution of various installation activities, it is important to find the operational limits in the design phase. In practice, the installation activities are executed in sequence and the success of the following activities normally depends on the previous step. Thus, the operational limits should be evaluated for each activity and in sequential order. This study first presented the installation procedure for the MP hammering process with sequentially defined activities as commonly used by offshore installation contractors. Using a coupled HLV–MP model, numerical analysis were performed in the time-domain for various conditions, from where the critical events and corresponding limiting parameters were identified. Finally, a systematic methodology to find the allowable sea states for such operation was proposed. This study provided realistic examples to find the allowable sea states in a systematic way for a typical MP installation. The main conclusions of this study with recommendations are provided as follows.

- Numerical analysis is essential to quantify the dynamic responses for the system, and time-domain simulations are normally required for complex coupled systems including nonlinearities. The time-domain simulations of the coupled HLV–MP system shows that the penetration depth of the MP and wave conditions greatly influence the dynamic responses. The slowly varying second-order motions dominate the system in short waves and shallow penetration depths. The natural modes and natural periods of the HLV–MP system change significantly with the penetration depth. Because of the high gripper and soil stiffness coefficients at deeper penetrations, the natural periods of the horizontal motions of the system reduce and the first-order resonant motions are enhanced in long waves.
- The critical event for the initial hammering process is identified to be the structural failure of the hydraulic cylinders on the gripper, while the restrictive event is the unacceptable MP inclination at the end of the process. The limiting parameters during the initial hammering process are identified as the cylinder contact force and the inclination of the MP, respectively.
- The hydraulic cylinder force increases significantly with MP penetration in all wave conditions and it is recommended to retract the hydraulic cylinder rods as soon as the MP reaches the critical penetration depth (d_{c1}) at which it can stand alone in waves. The critical depth d_{c1} can be obtained from available soil properties of the offshore site. The characteristic forces on the hydraulic cylinders can be used as design criteria. It is also recommended to monitor the forces on the hydraulic cylinders during the installation to avoid reaching the extreme forces.
- The cylinder forces and MP inclination when using a jack-up vessel were compared with the floating HLV–MP system. The observations from using a floating HLV are not applicable for the jack-up vessel. Therefore, the critical events and limiting parameters depend on the installation equipment and installation procedures.
- The sensitivity study using different soil properties shows that the system dynamic behavior is not sensitive to the soil properties, and the critical depths for allowable cylinder contact forces occur at different penetrations.
- A methodology to obtain the allowable sea states is proposed. It can be applied in the design phase using the results from time-domain analysis and the allowable limits. The extreme hydraulic cylinder forces over 3 hrs are estimated using mean upcrossing rates while the inclinations of the MP are taken as the maximum over 10 min. The allowable values are taken from the commonly used design specification for the hydraulic systems and installation requirement for MP inclination. The allowable sea states can be used on-board together with weather forecasts to support decision-making.
- From the case studies, different unacceptable conditions can be identified. The reasons for those cases to happen were given and can be useful for future improvement of the installation

procedure, components design and contingency actions. It is recommended to reduce the second-order motions in short waves and to mitigate the first-order resonant motions in long waves.

- The proposed methodologies can be generalized for planning other marine operations.

7 Limitations and Future Work

This study describes a simplified installation procedure for MPs with a focus on the initial hammering process of the MP. Assumptions and simplifications are applied. The thruster capacity and mooring line tensions were assumed sufficient during the operation. No wind and current forces were applied. The soil models were simplified by distributed nonlinear springs. Furthermore, in practice there are many uncertainties associated with the measurements, inherent to the proposed methodology, numerical models, environmental conditions, etc. Future work can be devoted to address the above limitations.

This study provided the allowable sea states for the identified limiting parameters. It is also important to focus on improving the procedure and the system components related to those parameters to increase the allowable sea states. Possible solutions can be to upgrade the capacity of the hydraulic cylinders to increase the allowable limits or to use motion compensation system to reduce the motions of the coupled HLV–MP system for reducing the forces on the hydraulic cylinders.

In addition, the initial hammering activity is only one part of the group installation activities for MP installation. It is necessary to assess the allowable sea states of other individual activities, such as MP upending and lowering operations and combine them to establish the operational limits of the complete operation. The methodology will be generalized to other marine operations in order to establish their operational limits in a systematic way.

Acknowledgment

This work has been financially supported by the Research Council of Norway granted through the Department of Marine Technology, the Centre for Ships and Ocean Structures (CeSOS) and the Centre for Autonomous Marine Operations and Systems (AMOS), NTNU. The authors are grateful to Prof. Gudmund Eiksund from NTNU for valuable discussions on the modeling of the soil interaction forces, to Dr. Oleh Karpa from NTNU for providing the ACER tools to estimate extreme values using upcrossing rates, to Dr. Amir Nejad for providing insights on mechanical components, hydraulic systems and valuable discussions.

References

[1] EWEA, 2014, "The European Offshore Wind Industry—Key Trends and Statistics 2013," Report, The European Wind Energy Association, Brussels, Belgium.
[2] Thomsen, K., 2011, *Offshore Wind: A Comprehensive Guide to Successful Offshore Wind Farm Installation*, Academic Press, Waltham, MA.
[3] Ringsberg, J. W., Daun, V., and Olsson, F., 2015, "Analysis of Impact Loads on a Self-Elevating Unit During Jacking Operation," ASME Paper No. OMAE2015-41030.
[4] Sarkar, A., and Gudmestad, O., 2013, "Study on a New Method for Installing a Monopile and a Fully Integrated Offshore Wind Turbine Structure," Mar. Struct., **33**, pp. 160–187.
[5] Li, L., Gao, Z., and Moan, T., 2013, "Numerical Simulations for Installation of Offshore Wind Turbine Monopiles Using Floating Vessels," ASME Paper No. OMAE2013-11200.
[6] Li, L., Gao, Z., Moan, T., and Ormberg, H., 2014, "Analysis of Lifting Operation of a Monopile for an Offshore Wind Turbine Considering Vessel Shielding Effects," Mar. Struct., **39**, pp. 287–314.
[7] Li, L., Gao, Z., and Moan, T., 2015, "Comparative Study of Lifting Operations of Offshore Wind Turbine Monopile and Jacket Substructures Considering Shielding Effects," 25th International Offshore and Polar Engineering Conference, June 21–26, Kona, HI.
[8] Li, L., Gao, Z., and Moan, T., 2015, "Response Analysis of a Nonstationary Lowering Operation for an Offshore Wind Turbine Monopile Substructure," ASME J. Offshore Mech. Arctic Eng., **137**(5), p. 051902.
[9] Smith, C., 2014, Offshore Piles on the Straight and Narrow, Last accessed on July 15, 2015, http://www.nce.co.uk/news/geotechnical/offshore-piles-on-the-straight-and-narrow/8663331.article.
[10] Strandgaard, T., and Vandenbulcke, L., 2002, "Driving Mono-Piles Into Glacial Till," IBCs Wind Power Europe.
[11] DNV, 2011, "Marine Operations," General, Det Norske Veritas, Oslo, Norway, Offshore Standard DNV-OS-H101.
[12] MARINTEK, 2012, *SIMO—Theory Manual Version 4.0*, MARINTEK, Trondheim, Norway.
[13] Newman, J. N., 1974, "Second-Order, Slowly-Varying Forces on Vessels in Irregular Waves," International Symposium on the Dynamics of Marine Vehicles and Structures in Waves, University College, London.
[14] Lee, C., 1995, *WAMIT Theory Manual*, Department of Ocean Engineering, Massachusetts Institute of Technology, Cambridge, MA.
[15] DNV, 2010, "Environmental Conditions and Environmental Loads," Det Norske Veritas, Oslo, Norway, Recommended Practice DNV-RP-C205.
[16] Albers, P., 2010, *Motion Control in Offshore and Dredging*, Springer Science & Business Media, Verlag, Germany.
[17] Carswell, W., Johansson, J., Løvholt, F., Arwade, S., Madshus, C., DeGroot, D., and Myers, A., 2015, "Foundation Damping and the Dynamics of Offshore Wind Turbine Monopiles," Renewable Energy, **80**, pp. 724–736.
[18] Bisoi, S., and Haldar, S., 2014, "Dynamic Analysis of Offshore Wind Turbine in Clay Considering Soil Monopile Tower Interaction," Soil Dyn. Earthquake Eng., **63**, pp. 19–35.
[19] Andersen, L. V., Vahdatirad, M., Sichani, M. T., and Sørensen, J. D., 2012, "Natural Frequencies of Wind Turbines on Monopile Foundations in Clayey Soils a Probabilistic Approach," Comput. Geotech., **43**, pp. 1–11.
[20] Gerolymos, N., and Gazetas, G., 2006, "Development of Winkler Model for Static and Dynamic Response of Caisson Foundations With Soil and Interface Nonlinearities," Soil Dyn. Earthquake Eng., **26**(5), pp. 363–376.
[21] Ong, M., Li, H., Leira, B. J., and Myrhaug, D., 2013, "Dynamic Analysis of Offshore Monopile Wind Turbine Including the Effects of Wind–Wave Loading and Soil Properties," ASME Paper No. OMAE2013-10527.
[22] DNV, 2014, "Design of Offshore Wind Turbine Structures," Det Norske Veritas, Oslo, Norway, Offshore Standard DNV-OS-J101.
[23] API, 2007, "Recommended Practice for Planning, Designing and Constructing Fixed Offshore Platforms Working Stress Design," American Petroleum Institute, Washington DC, API Recommended Practice 2A-WSD (RP 2A-WSD).
[24] Byrne, B., McAdam, R., Burd, H., Houlsby, G., Martin, C., Zdravkovi, L., Taborda, D., Potts, D., Jardine, R., and Sideri, M., 2015, "New Design Methods for Large Diameter Piles Under Lateral Loading for Offshore Wind Applications," 3rd International Symposium on Frontiers in Offshore Geotechnics (ISFOG 2015), Oslo, Norway, June 10–12.
[25] Lesny, K., and Wiemann, J., 2006, "Finite-Element-Modelling of Large Diameter Monopiles for Offshore Wind Energy Converters," Geo Congress, Feb. 26–Mar. 1, Atlanta, GA.
[26] Hededal, O., and Klinkvort, R. T., 2010, "A New Elasto-Plastic Spring Element for Cyclic Loading of Piles Using the py Curve Concept," *Numerical Methods in Geotechnical Engineering*, Benz and Nordal, eds., Taylor & Francis Group, London, pp. 883–888.
[27] Bekken, L., 2009, "Lateral Behavior of Large Diameter Offshore Monopile Foundations for Wind Turbines," Ph.D. thesis, TU Delft, Delft University of Technology, Netherlands.
[28] Lombardi, D., Bhattacharya, S., and Wood, D. M., 2013, "Dynamic Soil-Structure Interaction of Monopile Supported Wind Turbines in Cohesive Soil," Soil Dyn. Earthquake Eng., **49**, pp. 165–180.
[29] Vemula, N. K., de Vries, W., Fischer, T., Cordle, A., and Schmidt, B., 2010, "Design Solution for the Upwind Reference Offshore Support Structure, Deliverable D4.2.5," Technical Report, Project Upwind, WP4: Offshore Foundations and Support Structures.
[30] ANSYS, 2011, *The AQWA Reference Manual—Version 14.0*. ANSYS, Canonsburg, PA.
[31] Young-Kwan Kim, J.-R. S., and Yoon, D.-Y., 2012, "A Design of Windmill Turbine Installation Vessel Using Jack-Up System," 22nd International Offshore and Polar Engineering Conference, June 17–22, Rhodes, Greece.
[32] Naess, A., 1984, "Technical Note: On a Rational Approach to Extreme Value Analysis," Appl. Ocean Res., **6**(3), pp. 173–174.
[33] Naess, A., 1984, "On the Long-Term Statistics of Extremes," Appl. Ocean Res., **6**(4), pp. 227–228.
[34] Naess, A., Gaidai, O., and Teigen, P. S., 2007, "Extreme Response Prediction for Nonlinear Floating Offshore Structures by Monte Carlo Simulation," Appl. Ocean Res., **29**(4), pp. 221–230.
[35] IHC, 2015, "IHC Vremac Cylinders—Cylinder Catalogue 210 bar /300 bar," Last accessed: May 05, 2015, http://www.ihcvremaccylinders.com/